

PNNL-38358 Rev 0
WTPSP-RPT-256 Rev 0

FY25 Task 5: Small-Scale Mixing

October 2025

Austin A Bachman
Amy M Westesen
Richard C Daniel
Carolyn M Burns
Edgar C Buck
Reid A Peterson

DISCLAIMER

This report was prepared as an account of work sponsored by an agency of the United States Government. Neither the United States Government nor any agency thereof, nor Battelle Memorial Institute, nor any of their employees, makes **any warranty, express or implied, or assumes any legal liability or responsibility for the accuracy, completeness, or usefulness of any information, apparatus, product, or process disclosed, or represents that its use would not infringe privately owned rights.** Reference herein to any specific commercial product, process, or service by trade name, trademark, manufacturer, or otherwise does not necessarily constitute or imply its endorsement, recommendation, or favoring by the United States Government or any agency thereof, or Battelle Memorial Institute. The views and opinions of authors expressed herein do not necessarily state or reflect those of the United States Government or any agency thereof.

PACIFIC NORTHWEST NATIONAL LABORATORY
operated by
BATTELLE
for the
UNITED STATES DEPARTMENT OF ENERGY
under Contract DE-AC05-76RL01830

Printed in the United States of America

Available to DOE and DOE contractors from
the Office of Scientific and Technical Information,
P.O. Box 62, Oak Ridge, TN 37831-0062
www.osti.gov
ph: (865) 576-8401
fox: (865) 576-5728
email: reports@osti.gov

Available to the public from the National Technical Information Service
5301 Shawnee Rd., Alexandria, VA 22312
ph: (800) 553-NTIS (6847)
or (703) 605-6000
email: info@ntis.gov
Online ordering: <http://www.ntis.gov>

FY25 Task 5: Small-Scale Mixing

October 2025

Austin A Bachman
Amy M Westesen
Richard C Daniel
Carolyn M Burns
Edgar C Buck
Reid A Peterson

Prepared for
the U.S. Department of Energy
under Contract DE-AC05-76RL01830

Pacific Northwest National Laboratory
Richland, Washington 99354

Acknowledgments

The authors gratefully acknowledge the financial support provided by Bechtel National, Inc. We are thankful to Johnathon Reyff and John Julyk for their oversight and collaboration.

The following Pacific Northwest National Laboratory staff members are acknowledged for their contributions: Renee Russell and Krusha Bhakta for technical review of the report and calculations, David MacPherson and Alyssa Peterson for quality assurance, Matt Wilburn for his technical editing contribution, Chrissy Charron and Cassie Martin for programmatic support during this work, and Reid Peterson for project management.

All of the PNNL shielded facilities operations staff helping in the laboratory to complete this work are greatly appreciated and acknowledged: Hollan Brown, Austin Forsyth, and Michael Rojas.

Acronyms and Abbreviations

| | |
|----------|---|
| DOE | U.S. Department of Energy |
| HB | high bound |
| MFPV | melter feed preparation vessel |
| N_{js} | just-suspended impeller speed |
| NQAP | Nuclear Quality Assurance Program |
| PNNL | Pacific Northwest National Laboratory |
| UDS | undissolved solids |
| WTP | Hanford Tank Waste Treatment and Immobilization Plant |

Quality Assurance

This work was performed in accordance with the Pacific Northwest National Laboratory (PNNL) Nuclear Quality Assurance Program (NQAP). The NQAP complies with the DOE Order 414.1D, *Quality Assurance*, and 10 CFR 830, Subpart A, *Quality Assurance Requirements*. The NQAP uses NQA-1-2012, *Quality Assurance Requirements for Nuclear Facility Applications*, as its consensus standard and NQA-1-2012, Subpart 4.2.1, as the basis for its graded approach to quality. The NQAP works in conjunction with PNNL's laboratory-level Quality Management Program, which is based on the requirements as defined in the DOE Order 414.1D and 10 CFR 830, Subpart A.

The work of this report was performed at a technology readiness level of 5, the highest level of applied research under NQAP.

Contents

| | |
|---|-----|
| Acknowledgments..... | iii |
| Acronyms and Abbreviations | iv |
| Quality Assurance..... | v |
| 1.0 Introduction..... | 1.1 |
| 2.0 Materials and Methods..... | 2.1 |
| 3.0 Results..... | 3.1 |
| 3.1 Critical Velocity vs. N_{js} | 3.1 |
| 3.2 Bench-Scale Simulant Testing..... | 3.2 |
| 3.3 Small-Scale Simulant Testing..... | 3.4 |
| 3.4 Actual Waste Testing..... | 3.5 |
| 4.0 Conclusions..... | 4.7 |
| 5.0 References..... | 5.1 |
| Appendix A – Tank Waste Information..... | A.1 |

Figures

| | |
|---|-----|
| Figure 2.1. Small-scale tank (left) and bench-scale tank containing melter feed preparation vessel simulant (right)..... | 2.1 |
| Figure 2.2. Cole-Parmer 316 stainless steel three-blade propeller, 1-1/2 in. diameter x 5/16 in. bore diameter (left), and IKA R 1345 propeller 4-bladed stirrer (right)..... | 2.2 |
| Figure 3.1. XL SciTech glass beads N_{js} vs. critical velocity (correlations from this data should not be extrapolated to N_{js} testing geometries other than that of the bench-scale system)..... | 3.2 |
| Figure 3.2. Bench-scale simulant N_{js} results as a function of the Zwietering constant (S)..... | 3.3 |
| Figure 3.3. Small-scale simulant N_{js} results as a function of S..... | 3.4 |
| Figure 3.4. Small-scale simulant and actual tank waste N_{js} results as a function of S | 3.6 |

Tables

| | |
|---|-----|
| Table 2.1. Mixing tank and baffle dimensions..... | 2.2 |
| Table 3.1. Density and particle size info for XL SciTech S1-D1, S1-D2, and S2-D2 glass beads | 3.1 |
| Table 3.2. Compositing strategies to combine 22 of the received waste jars. | 3.5 |

1.0 Introduction

The U.S. Department of Energy (DOE) Hanford Site has 177 underground storage tanks that contain a complex and diverse mix of chemical and radioactive wastes from past nuclear fuel reprocessing and waste management operations. The strategy of the DOE Hanford Field Office is to retrieve this waste, ~20 vol% of which is in the form of insoluble undissolved solids (UDS) or sludge, and treat it via immobilization at the Hanford Tank Waste Treatment and Immobilization Plant (WTP). The diverse properties and characteristics of Hanford tank waste are anticipated to lead to major challenges related to its transport from the underground tanks to the WTP. These challenges, however, can be addressed by investigating the behavior of tank waste samples and simulant materials and evaluating their behavior against the capabilities of mixing and transport system designs that may be incorporated to retrieve and treat the waste.

One challenging requirement relates to the UDS composition in a waste feed because the solid particles settle, and their concentration and relative proportion can change during batch transfers of the waste to the WTP. A key uncertainty is the ability to mix and transfer waste with large variations in UDS concentrations/solids compositions that result in wide ranges of physical properties such as settling rates, mixing and transport properties. To address this uncertainty, bench-scale mixing and settling tests have been conducted to determine the process performance for various physical and chemical properties of both actual Hanford tank waste sludge and simulant samples. Settling velocity, chemical characterization, shear strength measurements, and just suspended impeller speed (N_{js}) were determined for tank waste simulants and actual Hanford tank waste sludges to evaluate the mobilization of non-cohesive particles at various laboratory scales.

The most direct method of investigating transport behaviors of simulants and actual tank waste sludge is critical velocity (deposition velocity) testing, in which slurry samples are pumped through a straight horizontal pipeline at varying speeds and observed to determine a minimum velocity required to prevent the deposition of particles on the bottom of the pipeline (Poloski et al. 2009). However, this method presents several challenges that make it unrealistic for investigating the transport behavior of actual Hanford tank waste, including the primary limitation of sample size. The volumes of actual tank waste sludge samples available for experimentation are typically on the order of hundreds of milliliters, which is not nearly enough to use for critical velocity testing.

Critical velocity depends on the geometry of the transport system and physical properties of the solids and carrier fluid that comprise the slurry (Oroskar and Turian 1980). A promising alternative to direct critical velocity testing is to use N_{js} testing in conjunction with already available critical velocity information (Bontha et al. 2010). Critical velocity and N_{js} are both measures of solid suspension behavior and rely on many of the same parameters, as can be seen in Eqs. (1.1) and (1.2). Eq. (1.1) shows the formula used to estimate critical velocity:

$$V_{OT} = \sqrt{gd \left(\frac{\rho_s}{\rho_f} - 1 \right)} \left[1.85 C_c^{0.1536} (1 - C_c)^{0.3564} \left(\frac{D}{d} \right)^{0.378} \left(\frac{\rho_f D \sqrt{gd \left(\frac{\rho_s}{\rho_f} - 1 \right)}}{\mu_f} \right)^{0.09} \chi^{0.3} \right] \quad (1.1)$$

where g = gravitational constant (m/s²)
 d = particle diameter (m)
 D = inner pipe diameter (m)
 ρ_s = coarse solid density (kg/m³)
 ρ_f = carrier fluid density (kg/m³)
 C_c = coarse particle volume fraction
 μ_f = carrier fluid dynamic viscosity (Pa*s)
 χ = hindered settling factor

Eq. (1.2), as given in Paul et al. (2004), accounts for similar slurry information and is used to estimate N_{js} :

$$N_{js} = S\nu^{0.1} \left(\frac{g(\rho_s - \rho_f)}{\rho_f} \right)^{0.45} X^{0.13} d^{0.2} D_i^{-0.85} \quad (1.2)$$

where D_i = impeller diameter (m)
 ν = kinematic viscosity (m²/s)
 X = solids wt%
 S = Zwietering constant, a function of tank and impeller geometry

N_{js} testing is advantageous because it can be performed at much smaller scales and requires significantly lower sample volumes. By conducting N_{js} testing of materials with known critical velocities, benchmarks can be developed and used as comparison points for further N_{js} testing. This method is a useful tool for “ranking” the difficulty of transporting given materials and provides a means to assess whether the planned mixing/pumping capabilities of the WTP are adequate.

2.0 Materials and Methods

The equipment used to perform mixing tests was quite simple. Two different mixing tanks were developed for testing at two different scales. The larger of the two is referred to herein as the “bench-scale” tank and the other is referred to as the “small-scale” tank. Each tank had its own set of baffles, similar in design, with one baffle at every 90 degrees in the tank. Figure 2.1 shows the two tanks with their baffles installed.



Figure 2.1. Small-scale tank (left) and bench-scale tank containing melter feed preparation vessel simulant (right).

The mixing tank apparatuses are similar but are not perfectly scaled versions of one another. In terms of materials of construction, the bench-scale tank is made of styrene acrylonitrile and the small-scale tank is made of polystyrene. The baffles each consist of four stainless steel plates mounted from the top, protruding a certain distance into the tanks. Both tanks have flat bottoms, but slightly different curvatures at the corners where the bottom meets the wall. The corners of the bench-scale tank are more rounded, while the corners of the small-scale tank are a bit sharper. The lowest point of the small-scale tank is in the very corners of the tank, while the lowest point of the bench-scale tank is its center.

These differences in material of construction and geometry do not affect the conclusions drawn herein, as N_{js} measurements are only compared within each mixing apparatus, but are worth noting for informational purposes. Table 2.1 presents the dimensions of the baffles and tanks.

Table 2.1. Mixing tank and baffle dimensions.

| Mixing Tank Scale | Bench | Small |
|--|-------|-------|
| Tank Dimensions | | |
| Tank diameter, mm | 156 | 64 |
| Tank height, mm | 172 | 71 |
| Impeller diameter to tank diameter ratio | 0.64 | 0.59 |
| Baffle Dimensions | | |
| Width, mm | 13.0 | 6.2 |
| Thickness, mm | 1.5 | 3.5 |
| Length, mm | 147.6 | 51.0 |
| Clearance from bottom of vessel, mm | 16.7 | 16.7 |
| Distance of baffle to vessel wall, mm | 3.3 | 3.3 |

Note: Small-scale tank – Model no. S-12753 from U-line.

To mix the various slurries, a Scilogex SCI120-S overhead stirrer was used in conjunction with a pitched blade impeller – one for each of the two mixing tanks. The bench-scale tank used a four-blade pitched blade impeller, while the small-scale tank used a three-blade pitched blade impeller, as shown in Figure 2.2.



Figure 2.2. Cole-Parmer 316 stainless steel three-blade propeller, 1-1/2 in. diameter x 5/16 in. bore diameter (left), and IKA R 1345 propeller 4-bladed stirrer (right).

Note that in Figure 2.2, the impellers are pitched in opposite directions to each other. Because both impellers were used with the same overhead stirrer that operates in only one direction, the shafts were rotated with angular velocities pointing down into the tank. With the bench-scale impeller, this resulted in up-pumping, while down-pumping occurred with the small-scale impeller. Down-pumping is generally considered better for solid suspension purposes, but this difference was a non-issue because the results from these experiments were only for comparative purposes within each system, and up-pumping still accomplished the intended goal.

To perform an N_{js} measurement, the impeller inserted in the overhead mixer was adjusted to a certain height above the bottom of the tank, as measured by an adhesive ruler applied to the outside of each tank. In the bench-scale tank, typical impeller heights ranged from 30 to 60 mm at increments of 10 mm, while

in the small-scale tank, the impeller was placed at heights of 20, 25, or 30 mm. After setting the impeller height in the bench-scale tank, the overhead mixer was set to an initial speed of nominally 50 rpm, which was increased by intervals of nominally 25 rpm every 10 min until the solids were observed to be fully suspended. For the small-scale system, the process for performing an N_{js} measurement was similar, but altered slightly for the larger range of impeller speeds covered. Small-scale tests began at nominally 100 rpm and increased by increments of 25 to 100 rpm at the discretion of the cognizant engineer. Specifically for the tests done in the hot cells, mixing began at a speed of 50 rpm and increased by 50 rpm every two minutes until nominally 500 rpm was reached. After this threshold was reached, the mixing speed was increased by increments of 10 rpm until full suspension was achieved.

Throughout each test, two cameras were used to record from the point just before the overhead mixer was turned on until the N_{js} measurement was determined to be complete. The cameras were simple Logitech webcams and were positioned with one at the side of the tank and one below. To get the bottom-side view, the mixing tanks were raised on a clear plastic stand, under which a camera could be placed.

3.0 Results

Three measurements were made during each N_{js} test: the rpm values at which top layer disturbance, bottom layer disturbance, and full suspension occurred. “Top layer disturbance” was defined as the first point at which any solids became suspended, often resulting in the liquid layer above the solids bed becoming cloudy and opaque. “Bottom layer disturbance” was defined as the point at which the first signs of movement of the solids on the bottom of the mixing tank were observed and was often indicated by a small area changing in coloration or observable motion of particles. “Full suspension” was defined as the state in which motion on the bottom of the tank indicated no more remaining settled solids, often accompanied by an observable swirling motion and more uniform coloration. The rpm value at which full suspension occurred was recorded as the N_{js} value. The primary focus during experimentation was the N_{js} value associated with each test condition.

3.1 Critical Velocity vs. N_{js}

N_{js} testing began with running experiments in the bench-scale mixing tank to show that N_{js} can effectively be used to evaluate the transport behavior of different materials. Three types of XL SciTech glass beads with varying densities and particle size characteristics were chosen for this purpose because of their previous use in critical velocity testing (Bontha et al. 2010). Table 3.1 shows density and particle size for the three bead types used.

Table 3.1. Density and particle size info for XL SciTech S1-D1, S1-D2, and S2-D2 glass beads.

| Bead | Nominal Density, g/mL | Particle Size (volume) $d(50)$, μm |
|-------|--------------------------|---|
| S1-D1 | 2.48 | 164.1 |
| S1-D2 | 2.48 | 69.1 |
| S2-D2 | 4.18 | 67.9 |

Looking at Eqs. (1.1) and (1.2), both critical velocity and N_{js} are dependent on density and particle size. For both equations, increases in density and particle size are expected to increase the resulting critical velocity and N_{js} value. Based on the values listed in Table 3.1 and their impact on Eqs. (1.1) and (1.2), it was expected that it would be easiest to suspend the S1-D2 beads, and the most difficult to suspend the S2-D2 beads, which is in line with the results from critical velocity testing by Bontha et al. 2010 and is further validated by the results shown in Figure 3.1.

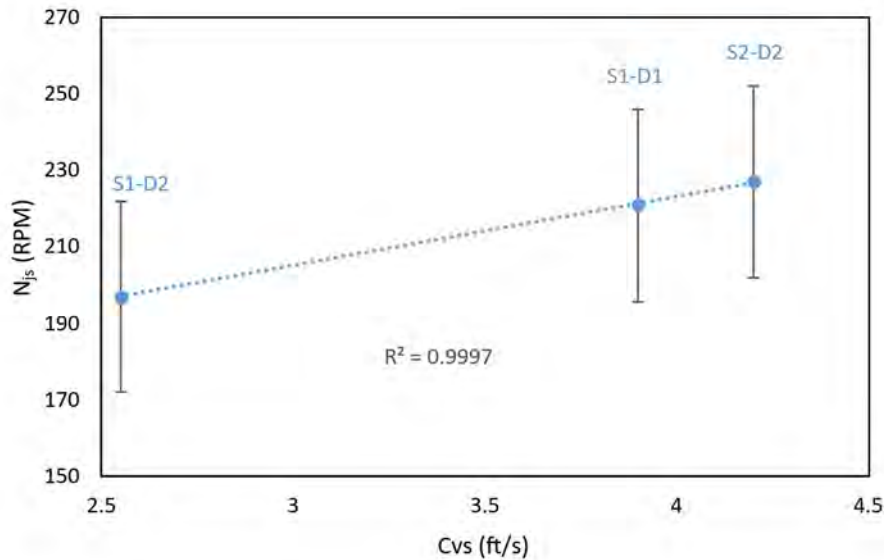


Figure 3.1. XL SciTech glass beads N_{js} vs. critical velocity (correlations from this data should not be extrapolated to N_{js} testing geometries other than that of the bench-scale system).

Critical velocity and N_{js} information were both collected using slurries of the glass beads in water, at a composition of 10% solids by mass. The N_{js} testing results for the XL SciTech glass beads (at an impeller height of 4 cm from the bottom in the bench-scale system) and their apparent relationship to critical velocity, shown in Figure 3.1, points toward a strong correlation between N_{js} and critical velocity, as indicated by the R^2 value of 0.9997. However, due to the methodology employed when making N_{js} measurements, there is some uncertainty associated with each N_{js} value. This is due to the increments by which the mixing speed was increased over the course of a test, which was generally ~ 25 rpm. Full suspension could therefore have been achieved anywhere between the mixing speed recorded as the N_{js} value and the penultimate mixing speed. The actual rotational speed of the overhead mixer is also not exact and was seen in testing to be 5-10 rpm below the displayed value when compared to a laser tachometer. This difference, however, remained consistent and should have minimal impact on the relative positions of the N_{js} measurements to one another.

Regardless of the uncertainty, N_{js} appears to be closely related to critical velocity and was pursued further, with several tank waste simulants ultimately investigated using the same equipment and methodology used for the glass beads. Gibbsite and boehmite simulants were chosen as these mineral phases are known to be present in actual tank waste, albeit at perhaps different particle size distributions. Iron oxide was chosen as a stand-in for some of the iron phases in actual tank waste, but may not represent the more amorphous phases adequately.

3.2 Bench-Scale Simulant Testing

Experiments were first performed in the “bench-scale” mixing tank apparatus. This tank was chosen based on its use by Westesen et al. 2023 in developing this specific capability. Several simulants were chosen for testing, including red iron oxide (Fe_2O_3), gibbsite [$Al(OH)_3$], boehmite (ALOOH), and a high-level waste melter feed preparation vessel (MFPV) simulant referred to as the “MFPV high hound (HB)” simulant. MFPV HB was developed by Eibling et al. 2003 for the purpose of providing a rheological upper bound and was used for large-scale mixing tests that had implications on the design of the WTP.

Figure 3.2 shows N_{js} results for these simulants tested at nominally 20 wt% solids in the bench-scale mixing apparatus.

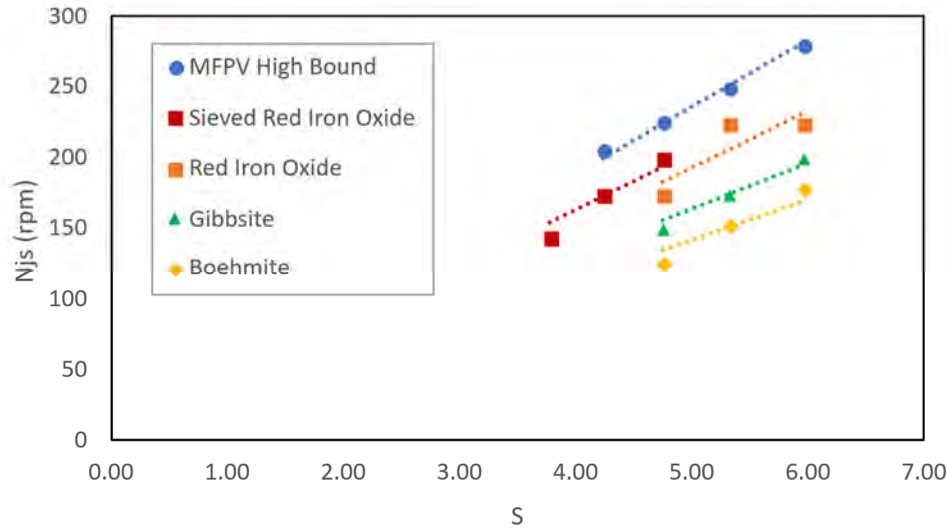


Figure 3.2. Bench-scale simulant N_{js} results as a function of the Zwieriing constant (S).

Figure 3.2 shows N_{js} as a function of the Zwieriing constant, S. The Zwieriing constant is a function of geometry, accounting for the ratio of the tank and impeller diameters and for the height of the impeller off the bottom of the tank, and was calculated using Eq. (1.2), as given in Armenente et al. (2008):

$$S = 1.78 * \left(\frac{T}{D}\right)^{1.16} * e^{(1.77 * \frac{C_b}{T})} \quad (3.1)$$

where T = tank diameter (mm)

D = impeller diameter (mm)

C_b = impeller distance off bottom (mm)

During all tests at the bench scale, the same mixing apparatus and same impeller were used, which means that S is reduced to being dependent on only the height of the impeller. The data shown in Figure 3.2 points to a linear relationship between S and N_{js} , which is predicted by the theoretical relationship given by Eq. (1.2) and suggests that the system is well-behaved.

Two of the simulants displayed in Figure 3.2 were selected because they are constituents of real Hanford tank waste: gibbsite and boehmite. N_{js} measurements tend to be dependent on the most difficult-to-suspend materials in the slurry, and as such, choosing a material known to exist in tank waste with the highest relative N_{js} would theoretically be the most effective route. However, it is not necessarily known what material/phase might be the most challenging, as that is what is being investigated. Gibbsite and boehmite are plentiful in tank waste, and thus these materials were anticipated to provide good benchmarks for what to expect when actual waste was later investigated.

Looking at the data displayed in Figure 3.1 and Figure 3.2 gives useful insight into the critical velocity that might be expected for tank waste. The S1-D2 beads at 10 wt% were found to have an N_{js} of 197 and a measured critical velocity of 2.55 ft/s, the lowest of the glass beads, as demonstrated in a test loop by Bontha et al. 2010. An N_{js} of 150 in the same configuration was measured for gibbsite at 20 wt%, which is significantly lower than the measurement for S1-D2. This indicates that gibbsite at a composition of 20

wt% UDS should have a critical velocity well below 2.55 ft/s, which would be easily within the operating velocity of the WTP (6 to 10 ft/s) recommended by Poloski et al. (2009). Assuming that gibbsite does in fact make for a reasonable tank waste simulant, this information supports the belief that the capabilities of the WTP should be adequate.

Interestingly, the three types of glass beads mentioned in Section 3.1 showed less ideal behavior than the other simulants in terms of the effect impeller height had on N_{js} . S1-D1 even showed the highest N_{js} occurring at the lowest S value, and the lowest N_{js} occurring at the highest S value – exactly the reverse of what is expected. This could possibly be the result of unexpected flow patterns in the bench-scale system, but it seems more probable that deviations from the hypothesized trend could be due to experimental uncertainty. It is likely worth repeating these experiments to reduce this uncertainty, especially considering that S1-D2 and S2-D2 are characteristically very similar to S1-D1 and showed the general positive correlation between N_{js} and S that is to be expected.

3.3 Small-Scale Simulant Testing

Bench-scale testing made for a good starting point for evaluating N_{js} but ultimately would not be feasible for testing real waste due to one of the same issues with critical velocity testing: limited sample sizes. While the sample required for performing a bench-scale N_{js} test is relatively small at ~2 L, most Hanford tank waste sludge samples acquired for testing are only a few hundred milliliters at best. Hence, a smaller apparatus for performing N_{js} tests was developed that only required around 100 to 150 mL of sample.

The main goal of bench-scale testing was to show that N_{js} measurements behaved in the manner hypothesized, in accordance with Eq. (1.2). On the other hand, small-scale testing was performed with the goal of creating benchmarks that could be used for comparison with actual tank waste measurements. Figure 3.3 shows the results of N_{js} measurements at the small scale.

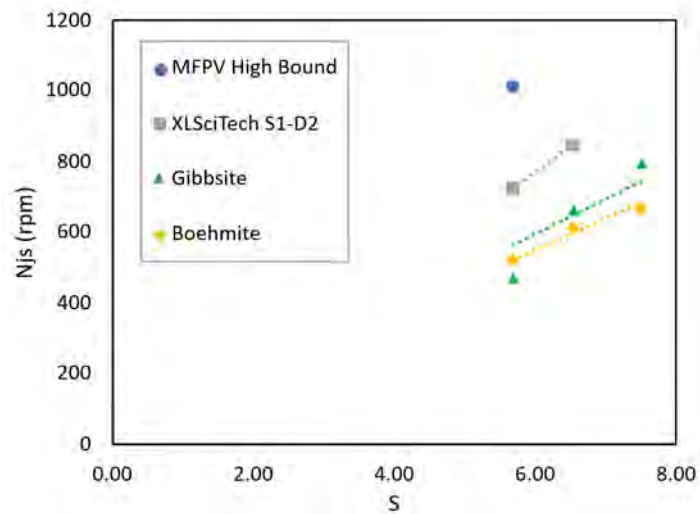


Figure 3.3. Small-scale simulant N_{js} results as a function of S .

Once again, the N_{js} measurements behaved mostly as predicted, including the measurements being significantly higher due to the decrease in tank and impeller diameters. Ideally, the results for gibbsite and boehmite at the small-scale would not cross over each other as they do in Figure 3.3, but the trends between measurements for each given material are reasonable – especially given that there is more uncertainty with each measurement, as the increments between rpm changes were larger for the small-scale tests.

Most important from the small-scale N_{js} data are the data points for the MFPV HB simulant and XL SciTech S1-D2 beads. The S1-D2 beads provide a good lower end reference point with a critical velocity of 2.55 ft/s, but the MFPV HB simulant provides a potentially more interesting reference point. This simulant was used for large-scale mixing testing and was formulated to be the “high bound” for what can be expected to transport through the WTP. So, any material with more difficult transport characteristics than the MFPV HB simulant can be assumed to pose challenges to the capabilities of WTP. Gibbsite and boehmite fell below both the MFPV HB simulant and S1-D2 beads, as shown in Figure 3.3, which indicates that at least these two components of actual tank waste should not be problematic to WTP.

3.4 Actual Waste Testing

After bench-scale and small-scale testing of the simulants, the next task was to test actual waste in the small-scale configuration. In the summer of 2024, a total of 24 jars of waste sludge from Hanford tanks AN-101, AN-106, and AW-105 were received in the Radiochemical Processing Laboratory at Pacific Northwest National Laboratory for rheometric characterization and transport property evaluation. Table A.1 presents information regarding the sample IDs as well as the tank and core segment from which each sample originated (Buck 2025). Twenty-two of these samples were combined to generate five composites, each with unique chemistry and enriched in a certain compound:

- Natrophosphate – termed the PO_4 composite
- Clarkeite – termed the U composite
- Gibbsite – termed the Al composite
- Iron – termed the Fe composite
- Zirconium – termed the Zr composite

The remaining two jars were kept for other project work. The strategies used for compositing and the composition of diluents used for achieving 20 wt% UDS can be found in Table 3.2 and Appendix A, respectively.

Table 3.2. Compositing strategies to combine 22 of the received waste jars.

| Composite | Jars to Combine |
|-------------------------|--|
| PO_4 Composite | 21378, 21417, and 21314 |
| U Composite | 21403, 21402, 21404, 21407, 21360, and 21366 |
| Al Composite | 21415, 20913, 20918, 21006, and 21315 |
| Fe Composite | 21416, 21357, and 21367 |
| Zr Composite | 19257, 20326, 19262, 20507-1, and 20507-2 |

Once the samples were composited to 20 wt%, each one underwent N_{js} testing in the small-scale mixing tank. The results from these tests are depicted in Figure 3.4, alongside the results from some of the simulant testing that helps put the N_{js} values for the actual tank waste in perspective.

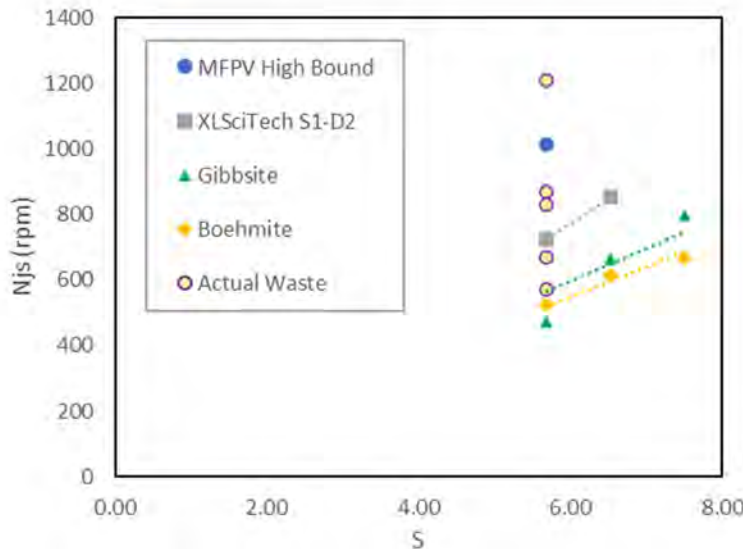


Figure 3.4. Small-scale simulant and actual tank waste N_{js} results as a function of S

In Figure 3.4, the various tank waste composites tested for off-bottom suspension are shown in ascending order of associated N_{js} behavior as follows: Al, U, PO_4 , Zr, and Fe. This indicates that the Al composite would have the lowest critical velocity, the Fe composite would have the highest, and the other samples would fall in between.

Unfortunately, a material with a known critical velocity that provided an upper bound for the actual waste samples was not tested in the small-scale system. A material such as this would have provided a more definitive idea of what critical velocities could be expected from all of the materials tested but is not necessary for the findings herein to be valuable. The XL-SciTech S1-D2 beads serve as a bounding material for at least the Al and U composites – the samples that were found to have N_{js} values lower than that of S1-D2. Because they fall below S1-D2, the critical velocity of the Al and U samples can be presumed to be below 2.55 ft/s – well below the recommended operational range of 6 to 10 ft/s.

Although a material with a known critical velocity that bounds all the actual waste samples was not tested, the MFPV HB simulant, developed by Eibling et al. (2003) specifically according to bounding rheological conditions outlined for the WTP, provides a valuable reference point for evaluating the transport characteristics of the materials with N_{js} values above that of S1-D2. These materials theoretically have critical velocities higher than 2.55 ft/s, but that does not necessarily indicate that they approach the limits of the WTP capabilities. As previously mentioned, MFPV HB was developed by Eibling et al. 2003 to represent the rheological upper bound of material received by the WTP and was used for large-scale mixing experiments that had implications for the design of WTP. This means that as long as the WTP is capable of processing MFPV HB, actual waste materials with N_{js} values less than that of MFPV HB can be expected to pose no issues from a critical velocity perspective.

However, not all of the composites were found to have N_{js} values less than that of MFPV HB. The Fe composite yielded an N_{js} value of 1210 rpm, which is significantly higher than the N_{js} value of 1014 found in the same testing configuration for MFPV HB. This indicates that if actual tank waste were composited in a similar manner to this Fe sample, it would not be bound by the MFPV HB simulant.

4.0 Conclusions

The complex and diverse constituents of Hanford tank waste are likely to pose significant challenges in terms of their transfer to the WTP. A key parameter of any waste to be transferred that must be understood is its critical velocity, so as to prevent the deposition of solids in pipelines, which can lead to plugging. Performing critical velocity testing of actual tank waste samples is not feasible due to the large sample volumes required, so N_{js} testing was used as a tool instead to correlate solid suspension behavior with critical velocity behavior.

XL-SciTech S1-D1, S1-D2, and S2-D2 were first tested in the bench-scale apparatus developed by Westesen et al. (2023) to evaluate the relationship between N_{js} and critical velocity behavior. These experiments revealed a strong correlation between the two, as shown in Figure 3.1, indicating that N_{js} testing can be used as an effective alternative to critical velocity testing.

Before actual tank waste samples were tested, the method of N_{js} testing was further evaluated for its sensitivity to changes in mixing geometry. Various simulants, including gibbsite, boehmite, and red iron oxide, were used for initial N_{js} testing, where the simulants were tested in the bench-scale mixing tank with the mixing impeller placed at different heights. There appeared to be a strong dependence of N_{js} on the Zwietering constant, S (a function of impeller height and tank geometry), as shown in Figure 3.2, which indicated that the N_{js} measurements were behaving as expected.

After bench-scale testing, a new, smaller test vessel was developed and denoted as the “small-scale” mixing vessel. Several of the same simulants were tested at the small scale, once again at different impeller heights to show the sensitivity of the N_{js} measurements. The N_{js} results demonstrated a dependence on impeller height similar to that at the bench-scale, but with a slightly weaker coefficient of determination.

Most importantly, benchmarks for actual waste testing were developed at the small-scale using XL SciTech S1-D2 glass beads and an MFPV HB simulant. The S1-D2 glass beads have a known critical velocity of 2.55 ft/s, and MFPV HB was used for large-scale mixing that had design implications for WTP. By obtaining N_{js} values for these two simulants, the N_{js} values of actual waste samples can be measured in the same configuration and then compared to that of the simulants, which makes it possible to predict what materials should have critical velocities within an acceptable range.

When the actual waste samples were tested in the same small-scale mixing apparatus, it was found that two of the composites (Al and U) had N_{js} values lower than that of S1-D2, and should therefore have critical velocities less than 2.55 ft/s. Two more composites (PO₄ and Zr) were found to have N_{js} values higher than that of S1-D2 but lower than MFPV HB. However, the Fe composite yielded the highest N_{js} value of all of the materials tested, including the MFPV HB. The MFPV HB simulant was developed to represent the upper bound of what would be received by the WTP, which combined with these results indicates that it cannot be confirmed from testing that the WTP will be capable of effectively handling all of the actual tank waste composites tested herein.

Further testing may need to be performed to evaluate the risk presented by different actual tank waste materials, and perhaps what makes the Fe composite the most challenging of the composites tested herein.

5.0 References

Bontha JR, HE Adkins, KM Denslow, JJ Jenks, CA Burns, PP Schonewill, GP Morgen, MS Greenwood, J Blanchard, TJ Peters, PJ MacFarlan, EB Baer, and WA Wilcox. 2010. *Test Loop Demonstration and Evaluation of Slurry Transfer Line Critical Velocity Measurement Instruments*. PNNL-19441 Rev. 0. Richland, WA: Pacific Northwest National Laboratory, U.S. Department of Energy.

Buck EC, AA Bachman, J Eshun, and RA Peterson. 2025. *Automated Particle Analysis of Hanford Tank Wastes 241-AN-106, 241-AN-101, and 241-AW-105*. PNNL-37622 Rev. 0 Richland, WA: Pacific Northwest National Laboratory, U.S. Department of Energy.

Eibling RE, RF Schumacher, EK Hansen. 2003. *Development of Simulants to Support Mixing Tests for High Level Waste and Low Activity Waste*. WSRC-TR-2003-00220, Rev. 0. Aiken, SC: Savannah River Site, U.S. Department of Energy.

Oroskar AR and RM Turian. 1980. *The critical velocity in pipeline flow of slurries*. *AIChE Journal* 26(4):550-558. <https://doi.org/10.1002/AIC.690260405>

Paul EL, VA Atiemo-Obeng, and SM Kresta. 2004. *Handbook of Industrial Mixing Science and Practice*. John Wiley & Sons, Inc., Hoboken, New Jersey.

Poloski AP, HE Adkins, J Abrefah, AM Casella, RE Hohimer, F Nigl, MJ Minette, JJ Toth, JM Tingey, and ST Yokuda. 2009. Deposition Velocities of Newtonian and Non-Newtonian Slurries in Pipelines. PNNL-17639; WTP-RPT-175, Rev. 0, Pacific Northwest National Laboratory, Richland, WA. <https://doi.org/10.2172/963206>.

Westesen, Amy M., Kyleigh J. Murray, Austin A. Bachman, Carolyn A. Burns, Trevor S. Scott, Jessica Rigby, and Reid A. Peterson. 2023. *Evaluation of High Level Waste Sludge Processing Behavior*. PNNL-35514. Richland, WA: Pacific Northwest National Laboratory.

https://www.pnnl.gov/main/publications/external/technical_reports/PNNL-35514.pdf

Zwietering, TN. 1958. *Suspending of solid particles in liquid by agitators*. Chemical Engineering Science 8(4), 244-253

Appendix A – Tank Waste Information

Table A.1. Received waste jars and their description

| Jar ID | Sample ID | Description |
|---------|------------|-------------------------|
| 21378 | S21R000250 | AN-101, Segment 13 LH |
| 21402 | S21T021171 | AN-101, Segment 12 LH |
| 21403 | S21T021172 | AN-101, Segment 12 UH |
| 21404 | S21T021201 | AN-101, Segment 13 UH |
| 21407 | S21T021230 | AN-101, Segment 14 UH |
| 21415 | S21T021675 | AN-101, Segment 18 LH |
| 21416 | S21T021676 | AN-101, Segment 18 UH |
| 21417 | S21T021747 | AN-101, Segment 19 LH |
| 20913 | S20T016919 | AN-106, Segment 14 |
| 20918 | S20T017242 | AN-106, Segment 15 UH |
| 21006 | S20T017241 | AN-106, Segment 15 LH |
| 21314 | S20T017587 | AN-106, Segment 16 LH |
| 21315 | S20T017588 | AN-106, Segment 16 UH |
| 21357 | S20T017662 | AN-106, Segment 18 UH |
| 21360 | S20T017884 | AN-106, Segment 19 LH |
| 21361 | S20T017885 | AN-106, Segment 19 UH |
| 21362 | S20T018179 | AN-106, Segment 20 UH |
| 21366 | S20T018217 | AN-106, Segment 21 UH |
| 21367 | S20T018254 | AN-106, Segment 22 UH |
| 19257 | S06T000221 | AW-105, Segment 8 LH |
| 19262 | S06T000220 | AW-105, Segment 8 UH |
| 20326 | S06T000217 | AW-105, Segment 8 LH |
| 20507-1 | S08T009997 | AW-105, Segment 8R2 CS1 |
| 20507-2 | S08T009997 | AW-105, Segment 8R2 CS2 |

Pacific Northwest National Laboratory

902 Battelle Boulevard
P.O. Box 999
Richland, WA 99354

1-888-375-PNNL (7665)

www.pnnl.gov